Acetylcholine-induced Calcium Signaling and Contraction of Airway Smooth Muscle Cells in Lung Slices

Albrecht Bergner and Michael J. Sanderson

Department of Physiology, University of Massachusetts Medical School, Worcester, MA 01655

ABSTRACT The Ca^{2+} signaling and contractility of airway smooth muscle cells (SMCs) were investigated with confocal microscopy in murine lung slices (~75-μm thick) that maintained the in situ organization of the airways and the contractility of the SMCs for at least 5 d. 10–500 nM acetylcholine (ACH) induced a contraction of the airway lumen and a transient increase in $[Ca^{2+}]_i$ in individual SMCs that subsequently declined to initiate multiple intracellular Ca^{2+} oscillations. These Ca^{2+} oscillations spread as Ca^{2+} waves through the SMCs at ~48 μm/s. The magnitude of the airway contraction, the initial Ca^{2+} transient, and the frequency of the subsequent Ca^{2+} oscillations were all concentration-dependent. In a Ca^{2+}-free solution, ACH induced a similar Ca^{2+} response, except that the Ca^{2+} oscillations ceased after 1–1.5 min. Incubation with thapsigargin, xestospongin, or ryanodine inhibited the ACH-induced Ca^{2+} signaling. A comparison of airway contraction with the ACH-induced Ca^{2+} response of the SMCs revealed that the onset of airway contraction correlated with the initial Ca^{2+} transient, and that sustained airway contraction correlated with the occurrence of the Ca^{2+} oscillations. Buffering intracellular Ca^{2+} with BAPTA prohibited Ca^{2+} signaling and airway contraction, indicating a Ca^{2+}-dependent pathway. Cessation of the Ca^{2+} oscillations, induced by ACH-esterase, halothane, or the absence of extracellular Ca^{2+} resulted in a relaxation of the airway. The concentration dependence of the airway contraction matched the concentration dependence of the increased frequency of the Ca^{2+} oscillations. These results indicate that Ca^{2+} oscillations, induced by ACH in murine bronchial SMCs, are generated by Ca^{2+} release from the SR involving IP_3- and ryanodine receptors, and are required to maintain airway contraction.

KEY WORDS: asthma • hyper-reactivity • confocal microscopy • Ca^{2+} oscillations • frequency modulation

INTRODUCTION

Our understanding of hyper-reactivity associated with asthma, which is the narrowing of airways induced by smooth muscle cell (SMC)* contraction, is assimilated from investigations of either whole airways (e.g., lung function tests or isolated airways) or from investigations of isolated single SMCs. Although studies with whole airways provide data about airway contraction, they provide little information regarding the underlying biological processes. By contrast, studies of isolated SMCs provide information regarding the cellular processes, but little information regarding the functional properties of the airway. The use of isolated SMCs has some additional drawbacks, including the tendency of the cells to de-differentiate and to lose contractility. For example, the response of cultured airway SMCs to stimulation via the muscarinic receptor subtype M3 that mediates SMC contraction by activating PLC and increasing intracellular Ca^{2+} concentration ($[Ca^{2+}]_i$) is reduced (Widdop et al., 1993; Hall and Kotlikoff, 1995).

To address some of these problems, we have refined the experimental use of lung slices. Lung slices previously have been used to study a variety of lung responses including bronchial contractility (Dandurand et al., 1993; Martin et al., 1996, 2000a,b, 2001; Salerno et al., 1996; Minshall et al., 1997; Duguet et al., 2000), vascular responses (Held et al., 1999), mucociliary function (Kurosawa et al., 1995), and allergic responses mediated by inflammatory cells (Dandurand et al., 1994; Wohlsen et al., 2001). Although most studies used video microscopy to document changes in airway size, the thickness of the slices precluded the observation of single cells. For example, Placke and Fisher (1987) and Dandurand et al. (1993) cut slices by hand that were 1,000–2,000-μm and 500–1,000-μm thick, respectively. Although Martin et al. (1996) reduced the slice thickness to ~250 μm using a tissue slicer, these slices remained unsuitable for single cell studies. With the aid of a vibratome tissue slicer, we have further reduced the slice thickness to ~75 μm and, using confocal microscopy, we were able to study individual cells in the lung slice.

Address correspondence to Michael J. Sanderson, Department of Physiology, University of Massachusetts Medical School, 55 Lake Avenue North, Worcester, MA 01655. Fax: (508) 856-5997; E-mail: michael.sanderson@umassmed.edu

*Abbreviations used in this paper: ACH, acetylcholine; $[Ca^{2+}]_i$, intracellular Ca^{2+} concentration; DMEM, Dulbecco's modified Eagle's medium; EC, epithelial cell; IP_3, inositol 1,4,5 trisphosphate; IP_3R, IP_3 receptor; MCH, methacholine; ROI, region of interest; sHBSS, supplemented Hanks' balanced salt solution; SMC, smooth muscle cell.

Agonist-induced increases in $[Ca^{2+}]_i$ frequently results in the stimulation of intracellular Ca^{2+} oscillations, and the idea arising from this correlation is that frequency-modulated Ca^{2+} signals regulate cellular activities (for reviews see Berridge et al., 2000; Bootman et al., 2001). In isolated tracheal SMCs, acetylcholine (ACH) has been found to induce an initial Ca^{2+} transient that was associated with an increase in SMC tension (Shieh et al., 1991). In the continued presence of ACH, this transient Ca^{2+} increase appeared to be followed by a reduced, but sustained, plateau in $[Ca^{2+}]_i$ that was sufficient for the maintenance of tension. Subsequent studies have revealed that the ACH-induced Ca^{2+} transient was actually followed by Ca^{2+} oscillations (Liu and Farley, 1996; Sims et al., 1996; Prakash et al., 1997, 2000; Sieck et al., 1997). However, these studies were performed on isolated tracheal SMCs, and the relationship of these Ca^{2+} transients and Ca^{2+} oscillations to airway caliber was unknown. Therefore, the correlation of the Ca^{2+} signaling in bronchial SMCs to airway contraction was the primary aim of the present study.

Cellular mechanisms of agonist-induced Ca^{2+} signaling in SMCs involve G-protein mediated activation of PLC, which hydrolyses phosphatidylinositol 4,5 bisphosphate to form diacylglycerol and inositol 1,4,5 trisphosphate (IP_3). IP_3 binds to specific receptors (IP_3R) within the SR and releases Ca^{2+} from the SR (for review see Bootman et al., 2001). However, the contribution of CICR from the SR via RYR and Ca^{2+} influx across the cell membrane varies among SMCs with respect to cell type and species (Savineau and Marthan, 2000). Therefore, the present study is also focused on the mechanisms involved in ACH-induced Ca^{2+} oscillations in murine SMCs of airways distal to the trachea.

In this study, we present a unique system using thin lung slices and confocal microscopy to study both the cellular Ca^{2+} signaling events in airway SMCs and the impact that this has on airway contraction. From our data, we suggest that ACH-induced Ca^{2+} oscillations in airway SMCs are generated by Ca^{2+} release from the SR involving IP_3R and RYR and that these Ca^{2+} oscillations are responsible for sustained SMC contraction and the associated reduced airway caliber. We also hypothesize that the magnitude of the sustained contraction may be regulated by the frequency of the Ca^{2+} oscillations.

MATERIALS AND METHODS

Materials

Cell culture reagents and plasticware were obtained from Invitrogen Life Technologies. Other reagents were obtained from Sigma-Aldrich unless otherwise stated. In most cases, the Hanks' balanced salt solution (sHBSS) was supplemented with 25 mM-HEPES buffer but lacked phenol red, unless otherwise stated.

Lung Slices

To cut thin lung slices, it was first necessary to stiffen and stabilize the soft lung tissue. This was achieved by inflating the lungs with liquid agarose that was subsequently induced to gel by reducing the temperature. A solution of 4% agarose (type VII-A: low gelling temperature) in distilled water was prepared at 60°C, cooled to 37°C, and mixed with 2× concentrated sHBSS with phenol red to give a 2% agarose-sHBSS solution at 37°C. Male BALB/C inbred strain mice (42–77 d old; Charles River Breeding Labs) were killed by intraperitoneal injection (12 ml/kg bodyweight Nembutal). The fur was rinsed with ethanol and the trachea was exposed. Sternotomy was performed and the chest wall was removed. Care was taken not to injure the lungs. To fill the lungs with agarose, the trachea was cannulated using an intravenous catheter system (model 20G Intima; Becton Dickinson). The inner needle was removed and the outer intravenous tube was secured with suture thread (Dexon II, 4–0; Davis and Geck). To allow the air trapped in the intravenous tube to escape, the tube was initially clamped next to the trachea and an unattached 20-gauge needle was inserted into the tube, distal to the clamp. Once the tube was filled with agarose-sHBSS using a syringe, the clamp was removed and the lungs were slowly inflated with agarose-sHBSS (~1 ml). To prevent premature gelling of the agarose, the mouse and associated equipment were kept warm with a heat lamp. Subsequently, 0.1–0.2 ml of air was injected to flush the agarose-sHBSS out of the airways. The intravenous tube was clamped again to prevent leakage. The lungs were rinsed with 4°C sHBSS and the mouse was placed at 4°C for 15 min. The lungs were removed, placed in 4°C sHBSS, and cooled for an additional 15 min to ensure the complete gelling of the agarose within the lungs. After isolating single lung lobes, slices of ~75-μm thickness were cut at 4°C in sHBSS with a tissue slicer (model EMS-4000; Electron Microscopy Sciences). Up to eight slices were placed in one petri dish and cultured by floating them in 2 ml of DMEM supplemented with 10% FBS and antibiotics and antimycotics at 37°C in 10% CO_2. The actual slice thickness was measured using a position servo controller (model LVPZT E-662; Physik Instrumente) mounted on a confocal microscope.

Immunohistochemistry

Slices were washed in sHBSS, fixed for 5 min in 100% acetone, and washed in sHBSS containing 10% FBS. Antibodies were diluted 1:100 in sHBSS with 10% FBS. The slices were incubated for 1 h at room temperature with monoclonal mouse anti–α-smooth muscle actin (product number A-2547; Sigma-Aldrich) or monoclonal mouse anti–pan cytokeratin (product number C-2562) antibodies. Slices were washed in sHBSS with 10% FBS, incubated for 1 h at room temperature with FITC-conjugated anti–mouse IgG (1:100 in sHBSS with 10% FBS), embedded in anti-fade solution (SlowFade; Molecular Probes), and inspected on a confocal microscope.

Measurement of Airway Contraction or Relaxation

Experiments were performed on lung slices containing airways cut in cross-section. Care was taken to select airways with a lumen that was free of agarose and completely lined by epithelial cells showing ciliary activity. The slices were placed on cover glasses within a custom made Plexiglas chamber, held in position by a nylon mesh (CMN-300-B; Small Parts Inc.) and observed with an inverted microscope (model Diaphot 300; Nikon) using a 20× objective. The bathing solution for all experiments was sHBSS. Phase-contrast images were recorded using a digital high speed CCD camera (model TM-6710; Pulnix America), a digital camera interface ("Road Runner"; BitFlow Inc.) and image acquisition

software ("Video Savant"; IO Industries Inc.). Frames were captured in time-lapse (1 frame/s), stored in TIF stacks of several hundred frames, and analyzed on a Pentium III computer using the image analysis software "Scion" (Scion Corporation; free download: www.scioncorp.com). After calibrating the image dimensions and setting an appropriate threshold to distinguish the lumen from the surrounding tissue, the area of the airway lumen was measured with respect to time by pixel summing. To emulate a line-scanning analysis of airway contraction, a single row of pixels, aligned across the lumen of the airway, was extracted from each frame within the image stack and aligned sequentially into a single image. Each analysis was performed using custom written macros.

Measurements of Intracellular Free Ca^{2+} Concentration

Slices were loaded for 1 h at room temperature with 20 μM Oregon green (Molecular Probes) in sHBSS containing 0.2% pluronic (Pluronic F-127; Calbiochem), 100 μM sulfobromophthalein, and 3 mg/ml ascorbic acid. After loading, the slices were incubated for at least 30 min in sHBSS containing 100 μM sulfobromophthalein and 3 mg/ml ascorbic acid to allow for complete dye deesterification. The bath solution for all experiments was sHBSS containing 3 mg/ml ascorbic acid (antioxidant to reduce bleaching).

Confocal microscopy was performed with a custom-built microscope (Sanderson and Parker, 2002) based on an inverted microscope. Briefly, the 488-nm line from an argon laser is scanned across the specimen with two oscillating mirrors (for X- and Y-scan). The resultant fluorescence (>510 nm) is detected by a photomultiplier tube. A video frame capture board digitizes the photomultiplier signal to form an image that is recorded to hard disc using the recording software "Video Savant." Images were recorded in time-lapse (1 or 4 frames/s, 420 pixels × 400 lines) or at high speed (60 frames/s, 420 pixels × 200 lines) for the detection of rapid changes. Regions of interest (ROI) of 10 × 10 pixels were defined in single SMCs. Average fluorescence intensities of an ROI were obtained, frame-by-frame, using a custom written macro. Bleach correction was calculated from the bleaching rate during a period of 15–30 s before the addition of drugs. Raw data were corrected with the bleach correction before a rolling average of three frames was calculated. Final fluorescence values were expressed as a fluorescence ratio (F/F_0) normalized to the initial fluorescence (F_0). Because the confocal system was not capable of recording transmitted phase-contrast images simultaneously with confocal fluorescence images, airway contraction was analyzed by measuring the area of the part of the airway lumen that was visible in the confocal images.

Drug Application

ACH chloride, ACH-esterase, and halothane were dissolved in sHBSS. A 10× solution was diluted to the final concentration by addition to the volume of the bath solution (e.g., 10 μl of 10^{-5} M ACH was added to 90 μl bath solution for a final concentration of 10^{-6} M ACH). BAPTA-AM, xestospongin (Calbiochem), ryanodine, and thapsigargin were dissolved in DMSO and diluted in sHBSS to the final concentrations used.

Statistics

Statistical analysis was performed using the one way repeated measurements analysis of variance (all pair-wise multiple comparison procedures = Student-Newman-Keuls method). A P value of $P < 0.05$ was considered statistically significant.

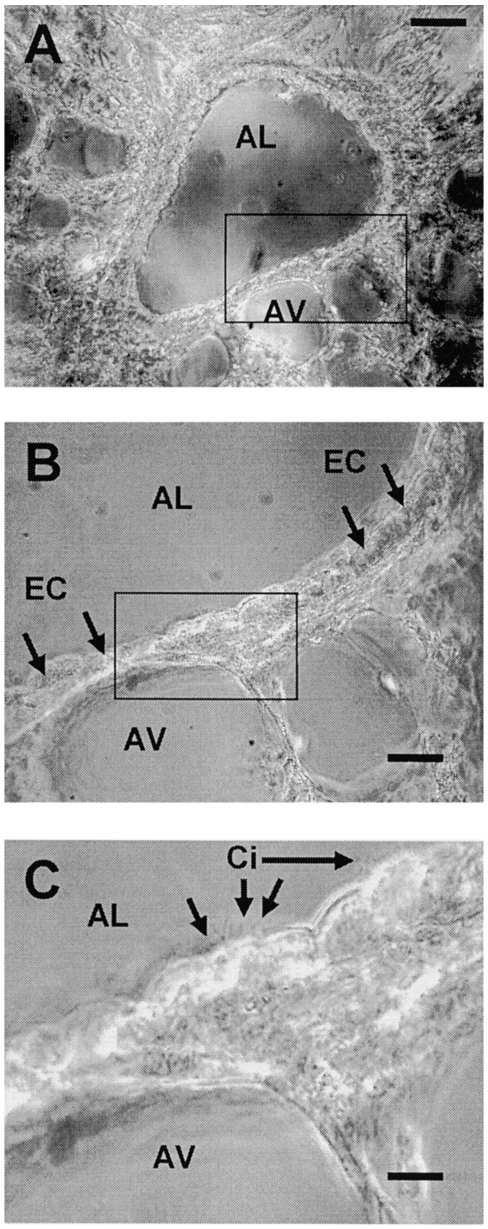

FIGURE 1. Phase-contrast images of a lung slice, ~75-μm thick, cut from agarose-filled murine lungs. (A) A low magnification image of a single airway in the lung slice. The airway is cut in cross-section and has a clearly visible lumen (AL). Several adjacent thin-walled alveoli (AV) are also evident. (B) A higher magnification view of the area outlined by the rectangle in A showing the epithelial cells (EC) that line the airway lumen. (C) A higher magnification of the area outlined by the rectangle in B showing the cilia (Ci) of the epithelial cells facing toward the airway lumen. Bars: (A) 50 μm; (B) 20 μm; (C) 8 μm.

RESULTS

Lung Slice Morphology and Properties

Agarose-filled murine lungs were cut into slices with a thickness of 73.3 ± 22.8 μm (mean ± SD, $n = 10$) using a vibratome tissue slicer. The slices were maintained by

floating them in culture medium to prevent adhesion to the dish and were found, as judged by conventional phase-contrast microscopy, to retain the normal morphological appearance and arrangement of the alveoli, blood vessels, and airways. Airways, cut in cross-section, could be easily identified and distinguished from blood vessels and alveoli based on a number of criteria. In contrast to blood vessels, the lumens of the airways were devoid of blood cells and were lined with cuboidal epithelial cells (ECs) that had clearly visible beating cilia (Fig. 1). The airways were relatively thick-walled in comparison to the numerous alveoli that formed thin-walled structures surrounding air spaces. Because of the extensive branching of the respiratory tract, airways were frequently cut at oblique angles. In the extreme case, a longitudinal section of an airway could be obtained. However, the same criteria, as described above, were applied to identify these airways.

To verify the morphological observations and to assess the spatial distribution of ECs and SMCs in the airways, we performed immunocytochemistry with antibodies specific for cytokeratin and α-smooth muscle actin, respectively. SMCs could be identified by their fusiform shape and were in many cases found around the whole circumference of the airway. However, in some airways, only parts of the circumference contained SMCs. SMCs were found to be closely associated with ECs, and were often separated from the airway lumen by just one layer of ECs (Fig. 2 A). By contrast, ECs showed a typical cobblestone-like appearance and completely lined the airway lumen (Fig. 2 B).

Because many airways were not cut precisely perpendicular, the cross-sections of the airways were not simple circular shapes (Fig. 1). As a result, the cross-sectional area is perhaps a more reliable measurement of airway size than the use of the diameter of the airway. The size of the airways in slices was measured with a CCD camera and image acquisition software. After the appropriate image calibration and the setting of a threshold to distinguish the lumen from the surrounding tissue, the cross-sectional area of the airways was calculated by pixel summing. The mean cross-sectional area of the airways found within a slice was 44,260 ± 6656 μm^2 (mean ± SD, $n = 48$) with a minimum value of 8,475 μm^2 and a maximum value of 112,088 μm^2. If a circular shape was assumed for all airways measured, the mean diameter would be 124 ± 92 μm (mean ± SD, $n = 48$) with an airway diameter range from 52 to 189 μm.

Morphology and contractility remained stable for at least 5 d in culture. Ciliary activity showed no apparent change for at least 10 d. After 10 d (without a change of culture medium), contractility decreased markedly and ciliary activity began to slow. As a result, experiments were performed only on slices 2–5 d old.

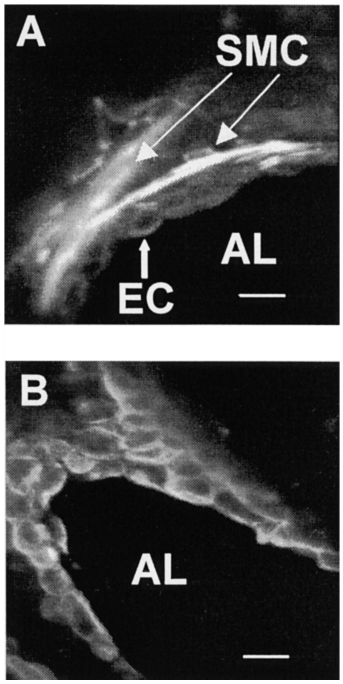

FIGURE 2. Confocal microscopy images of immunocytochemical stainings of airways in lung slices using FITC-conjugated secondary antibodies. (A) The wall of an airway, cut in cross-section, after staining with anti–α-actin antibodies. Several smooth muscle cells (SMC) stained brightly, show an elongated fusiform cell shape, and are in close spatial proximity to epithelial cells (EC) and airway lumen (AL). (B) A slice stained with anti–pan cytokeratin antibodies showing the typical cobblestone-like appearance of epithelial cells. In this case, the plane of the section has passed obliquely through the airway to provide near longitudinal section at the top left. Bars: 15 μm.

For the first few days after slice preparation, spontaneous airway contractions could be randomly observed (Fig. 3, before the addition of ACH). Unfortunately, a full systematic investigation of this phenomenon was hindered by its unpredictability. In lung slices of some mice, spontaneous contractions occurred in many airways, whereas in slices from other mice, no spontaneous activity could be observed at all. Similarly, the contractions ranged from "twitches" of parts of the airway wall without substantial change in airway lumen to contractions of the whole circumference, resulting in reduction of airway lumen of up to 50%. However, confocal microscopy did reveal that the spontaneous contractions occurred simultaneously with Ca^{2+} transients in SMCs. Whereas exposure to ACH-esterase ($n = 4$) or apyrase ($n = 3$) did not stop the contractions, exposure to a Ca^{2+}-free solution immediately stopped the spontaneous contractions ($n = 4$; unpublished data). These results suggest that an influx of external Ca^{2+} may play a role in the mechanisms responsible for spontaneous contractions. A detailed analysis of this phenomenon is beyond the scope of this work and will be the focus of future studies.

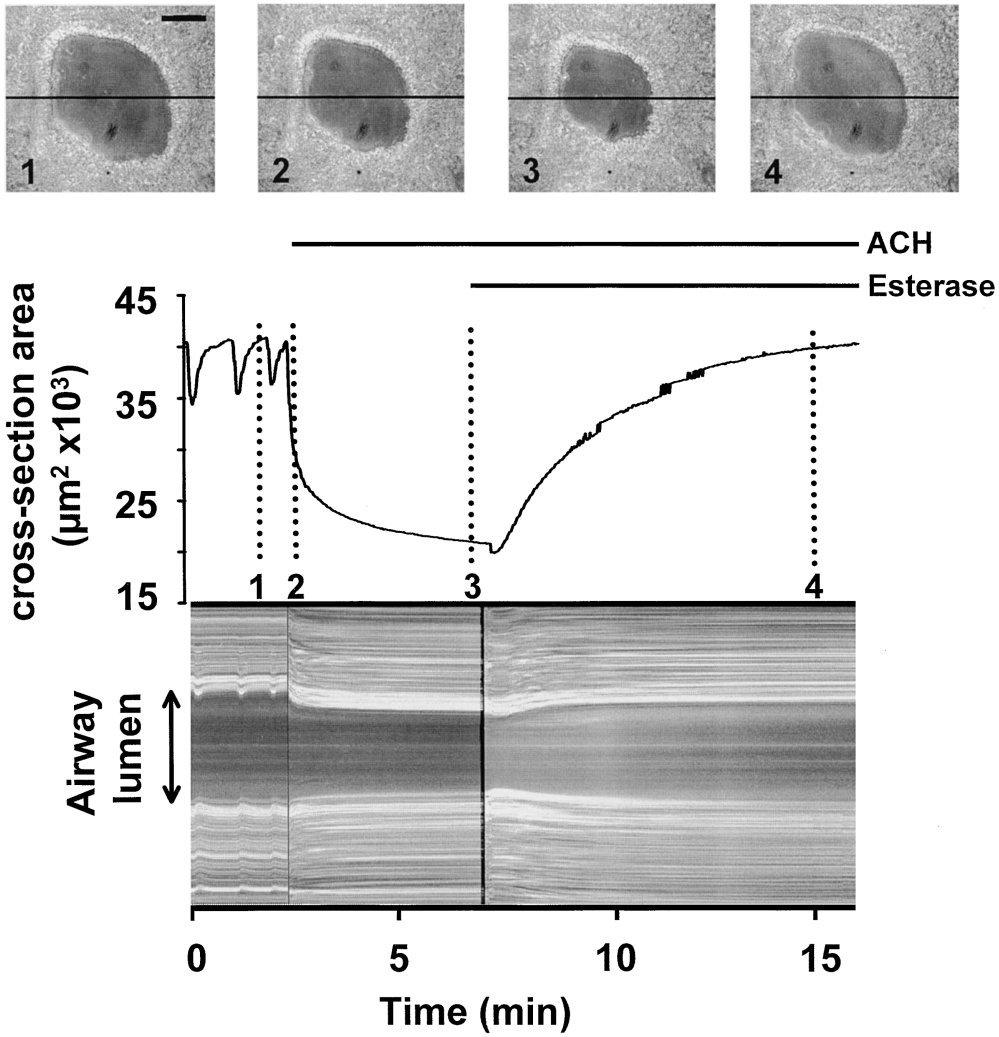

FIGURE 3. The change in the cross-sectional area of an airway in response to acetylcholine (ACH). An airway was monitored with phase-contrast microscopy and recorded in time-lapse at 1 frame/s in response to 1 µM ACH and 85 U/ml ACH-Esterase. (top, 1–4) Four images of the airway at different times (indicated by the dotted lines) showing the change in lumen size over 15 min. (middle) The cross-sectional area of the lumen was calculated and plotted against time. The airway displayed a number of spontaneous contractions followed by a large contraction in response to the application of ACH (bar). 1 µM ACH induced an airway contraction of ~50%. An initial steep phase of fast narrowing was followed by an asymptotic phase. The addition of 85 U/ml ACH-Esterase (bar) led to a short transient contraction followed by a relaxation of the airway back to baseline. (bottom) A line-scanning analysis of the airway responses induced by ACH and ACH-Esterase. Gray values of a single line across each image (black line in phase images 1–4) were sequentially aligned (vertically) to produce a 1-D temporal image of the activity. Trace is representative of eight experiments performed in eight different airways in eight different slices from two different mice. Bar: 50 µm.

ACH-induced Airway Contraction

Airway activity in slices was recorded in time-lapse at 1 frame/s using phase-contrast microscopy and the cross-sectional area was calculated for each frame. The addition of ACH, at concentrations >10 nM, induced airway contraction that reached a maximum contraction (or minimum cross-sectional area) within 5–10 min (Fig. 3). The effects of ACH were reversible by the degradation of ACH with ACH-esterase. A concentration dependence of the ACH-induced airway contraction could be observed in the range of 10–500 nM (Fig. 4). ACH-induced airway contraction was initiated by concentrations >10 nM, whereas concentrations >500 nM did not further decrease airway cross-sectional area (increased airway contraction). A complete closure of an airway was never observed. The addition of sHBSS alone had no effect on airway cross-sectional area.

ACH-induced Ca^{2+} Signaling

To load airway SMCs with sufficient dye, a high loading concentration (20 µM) of Oregon green was required in conjunction with the organic anion transport

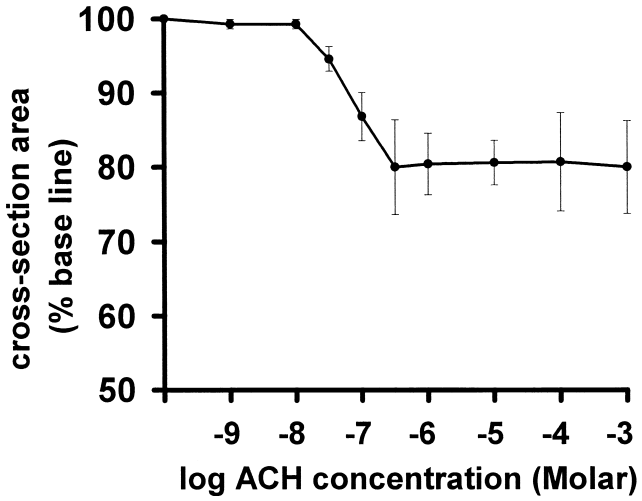

FIGURE 4. The concentration-response curve of ACH-induced airway contraction. Airways in lung slices were exposed to ACH and the minimum cross-sectional area was determined. A decrease in cross-sectional area occurs in the range of 10–500 nM. Concentrations of 1 μM or higher did not further decrease the minimum cross-sectional area, resulting in a plateau of contraction equal to ~80%. Each point represents five to eight experiments (mean ± SD) using a different airway in a different slice for each experiment. For each point, slices from at least two different mice were used.

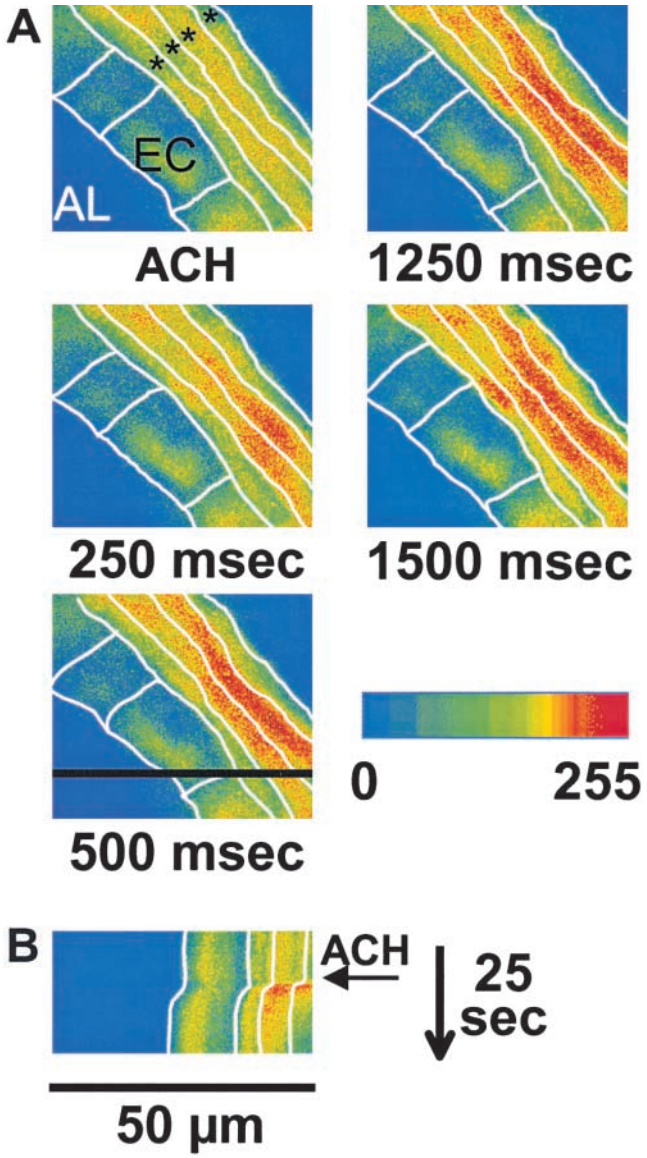

FIGURE 5. (A) A series of confocal pseudocolor images showing that epithelial cells (EC) separate the airway lumen (AL) from several adjacent smooth muscle cells (asterisks). In response to 1 μM ACH, the $[Ca^{2+}]_i$ is increased in the SMCs but not in the epithelial cells. Each SMC responds with a different time course. Time after the addition of ACH is indicated under each panel. White lines indicate the estimated cell boundaries. (B) A line-scan analysis of the effect of ACH. Intensity values from a single row (black line in image "500 ms") for each image recorded during 25 s were aligned into a single image. The arrow indicates the addition of ACH. ACH-induced airway contraction occurred simultaneously with the $[Ca^{2+}]_i$ increase.

blocker sulfobromophthalein (Di Virgilio et al., 1990). Using a custom-built confocal microscope (Sanderson and Parker, 2002), we were able to record and analyze Ca^{2+} signaling in contractile airway SMCs in the lung slices for 5 d after preparation. ROIs of 10 × 10 pixels were defined in SMCs and analyzed for Ca^{2+} changes.

The Ca^{2+} response to ACH consisted of an initial transient increase in $[Ca^{2+}]_i$ followed by Ca^{2+} oscillations (Figs. 5 and 6 A). By contrast, the $[Ca^{2+}]_i$ in ECs did not change in response to ACH. The addition of sHBSS alone had no effect. To evaluate the concentration dependence of the Ca^{2+} response, five SMCs in different slices were exposed to 10^{-8}, 10^{-6}, and 10^{-3} M ACH; a washout and a 20-min recovery period was allowed between each ACH exposure. The increase in $[Ca^{2+}]_i$ during the initial Ca^{2+} transient (the percent difference between the F/F_0 measured immediately before and at maximum value of the Ca^{2+} transient) was concentration-dependent from 10 nM to 1 mM (8.9 ± 15.2% for 10^{-8} M, 33 ± 31.8% for 10^{-6} M, and 73.1 ± 19% for 10^{-3} M; increase in percent of baseline, mean ± SD, $P < 0.05$, Fig. 6 B). The frequency of the Ca^{2+} oscillations (the average period of 10 sequential oscillations) at 10^{-6} M (25.2 ± 16.2 min^{-1}, mean ± SD) was higher than at 10^{-8} M (16.1 ± 17.5, $P < 0.05$) but did not differ between 10^{-6} and 10^{-3} M (28.4 ± 23.3; Fig. 6 C).

High speed recording of Ca^{2+} oscillations (60 frames/s) revealed that the oscillations spread as repetitive intracellular Ca^{2+} waves across the SMCs. The propagating velocity of the waves was calculated by defining 2 ROIs in the same cell and measuring the delay between the Ca^{2+} oscillations (velocity = distance between ROIs divided by delay between Ca^{2+} oscillations; Fig. 7 A) and was found to be 47.6 ± 9.2 μm/s (mean ± SD, $n = 3$). When the ROIs were defined in adjacent SMCs, the Ca^{2+} oscillations were asynchronous, indicat-

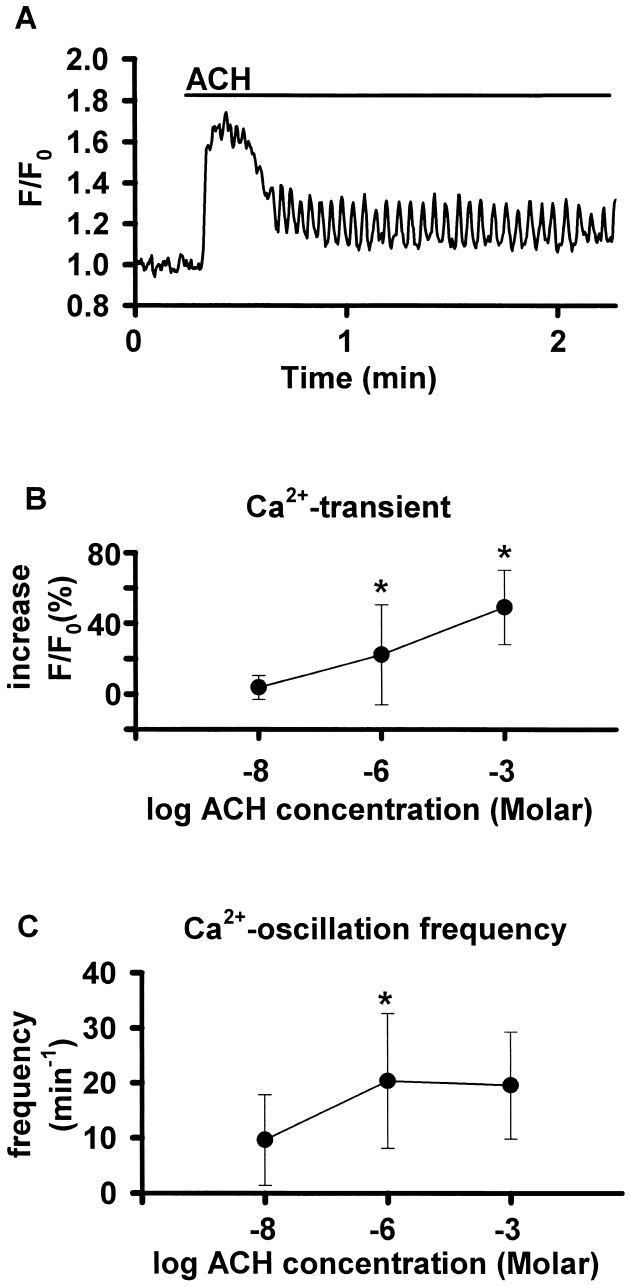

FIGURE 6. (A) Ca^{2+} signaling induced by ACH in airway SMCs in lung slices. ROIs were defined in SMCs and Ca^{2+} changes in response to 1 μM ACH (bar) expressed as a fluorescence ratio. The Ca^{2+} response consisted of an initial Ca^{2+} transient, followed by Ca^{2+} oscillations. (B and C) Concentration dependence of the Ca^{2+} response to ACH. Five SMCs in airways of different slices were exposed to 10^{-8}, 10^{-6}, and 10^{-3} M ACH with a washout and a 20-min recovery period between each exposure (*, $P < 0.05$). (B) The magnitude of the Ca^{2+} increase of the initial Ca^{2+} transient (the percent difference between the F/F_0 measured immediately before and at maximum value of the Ca^{2+} transient) was concentration-dependent. (C) The frequency of the oscillations (the average period of 10 sequential oscillations) at 10^{-6} M was higher than at 10^{-8} M, but did not differ between 10^{-6} and 10^{-3} M.

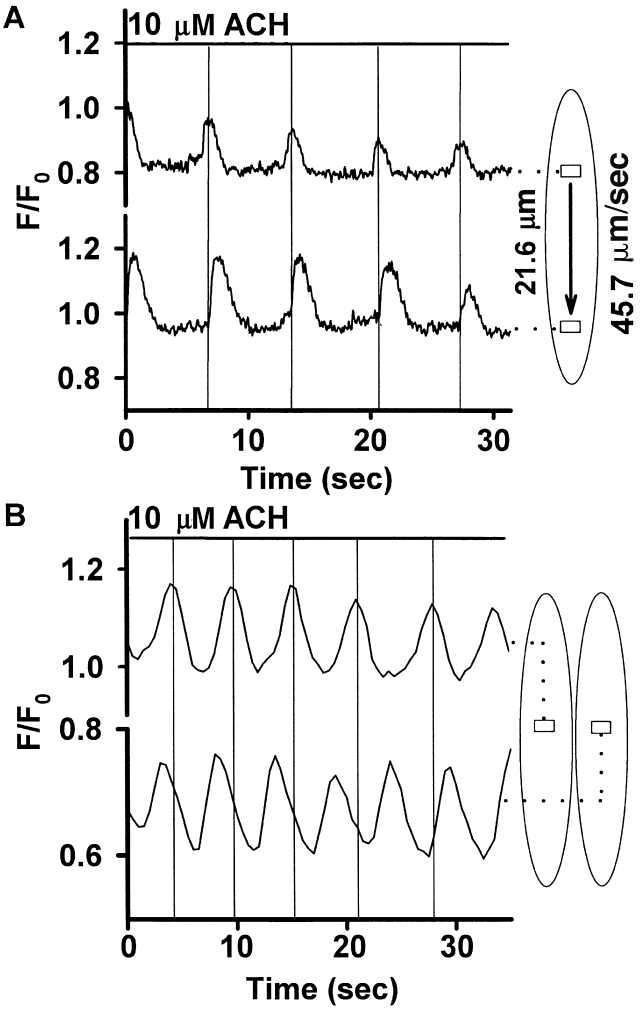

FIGURE 7. (A) Ca^{2+} oscillations as intracellular Ca^{2+} waves. Using confocal microscopy, ACH-induced Ca^{2+} oscillations were recorded at 60 frames/s. Two ROIs in the same SMC (21.6 μm apart) were analyzed, and ACH-induced Ca^{2+} oscillations displayed simultaneously. The Ca^{2+} oscillations of the two ROIs were phase-shifted, indicating a Ca^{2+} wave propagating through the cell. The temporal difference between the ROIs was 0.49 ± 0.11 s, giving a propagating velocity of the Ca^{2+} wave of 45.7 ± 11.1 μm/s for this cell ($n = 5$ consecutive oscillations, mean ± SD). Three similar experiments in three different SMCs in three different slices revealed an average propagating velocity of 47.6 ± 9.2 μm/s. (B) Ca^{2+} oscillations in ROIs in two adjacent cells were recorded and displayed simultaneously. The oscillations were asynchronous, indicating independent Ca^{2+} responses to ACH.

ing that adjacent SMCs have independent Ca^{2+} responses to ACH (Fig. 7 B).

To address the question, if Ca^{2+} influx from the extracellular space was involved in the generation of Ca^{2+} oscillations, we exposed airway SMCs to 10 μM ACH in a Ca^{2+}-free solution containing 5 mM EGTA. ACH induced Ca^{2+} oscillations, but these oscillations ceased after 1–1.5 min (Fig. 8 A). The inhibition of SR Ca^{2+}-ATPases with 10 μM thapsigargin for 30 min to empty intracellular Ca^{2+} stores prevented the Ca^{2+} increase in response to 10 μM ACH

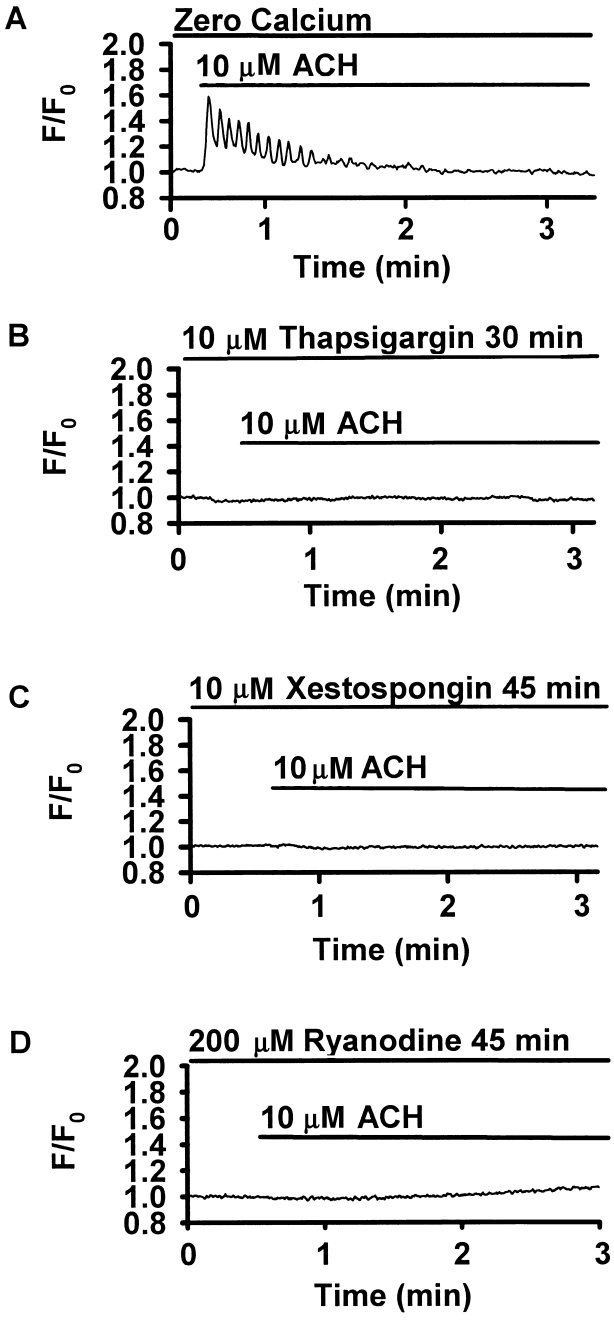

FIGURE 8. Mechanisms of ACH-induced Ca^{2+} oscillations. Traces are representative of four to five experiments performed in different airways of different slices obtained from at least two different mice. (A) In Ca^{2+}-free solution containing 5 mM EGTA, ACH-induced Ca^{2+} oscillations were initiated, but ceased after 1–1.5 min. (B) Incubation with 10 μM thapsigargin for 30 min abolished the Ca^{2+} response to ACH. (C) After a 45-min incubation with 10 μM xestospongin, no Ca^{2+} response to ACH could be detected. (D) Incubation with 200 μM ryanodine for 45 min also prevented the ACH-induced Ca^{2+} response.

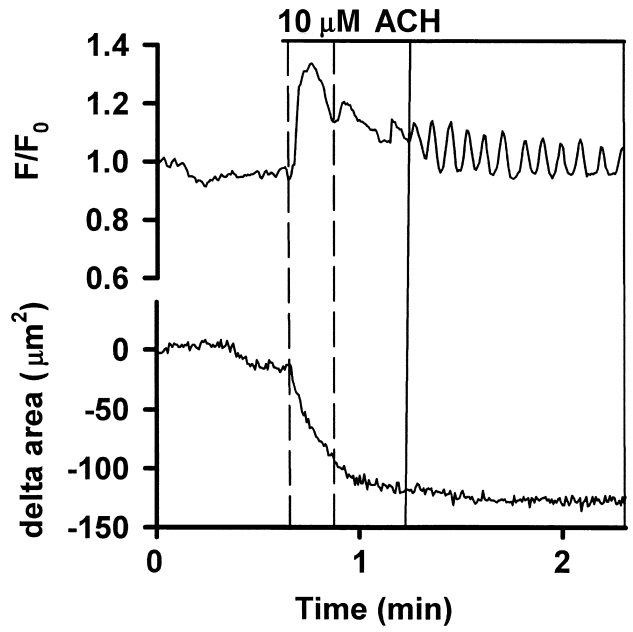

FIGURE 9. Correlation of ACH-induced Ca^{2+} signaling and airway contraction. ROIs were defined in single SMCs, and the Ca^{2+} changes in response to 10 μM ACH were expressed as a fluorescence ratio (top trace). The change in the part of the cross-sectional area of the airway that was visible in the confocal images was measured and displayed simultaneously as the delta area (bottom trace). The initial Ca^{2+} transient correlates with the airway contraction. The occurrence of the Ca^{2+} oscillations correlates with the maintenance of the reduced airway lumen. Representative traces of five experiments of five different airways in five different slices obtained from two different mice are shown.

(Fig. 8 B). Similarly, a 45-min incubation with 10 μM xestospongin or with 200 μM ryanodine inhibited the ACH-induced Ca^{2+} signaling (Fig. 8, C and D).

Correlation between Ca^{2+} Signaling in SMCs and Airway Contraction

A comparison of the Ca^{2+} response in SMCs with the corresponding airway contraction indicated that the Ca^{2+} transient occurred simultaneously with the initial contraction, whereas the Ca^{2+} oscillations occurred during the maintenance of the reduced airway lumen (Fig. 9). To test for the possibility that ACH may induce airway contraction by a Ca^{2+}-independent pathway, the intracellular Ca^{2+} was buffered by 1-h incubation with 1 mM BAPTA-AM. Upon exposure to 10 μM ACH, both the Ca^{2+} signaling and the airway contraction were abolished (Fig. 10 A). To investigate the relationship of the Ca^{2+} oscillations to sustained contraction, three different approaches were applied to inhibit ongoing Ca^{2+} oscillations without substantially changing the baseline $[Ca^{2+}]_i$. First, the degradation of ACH by 85 U/ml ACH-esterase abolished the Ca^{2+} oscillations and simultaneously relaxed the ACH-contracted airway (Fig. 10 B). Second, after the cessation of ACH-induced Ca^{2+} oscilla-

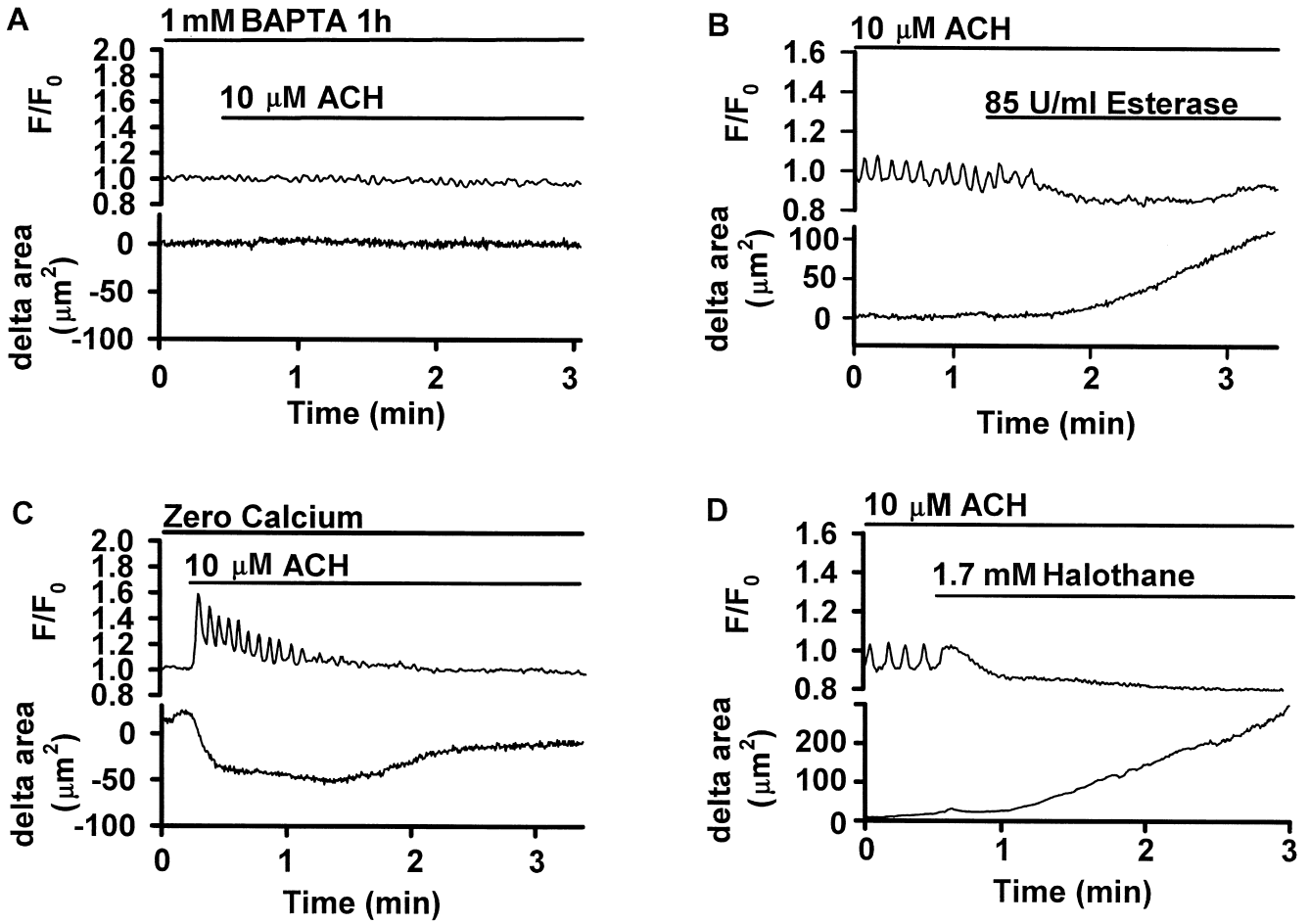

FIGURE 10. Ca^{2+} oscillations maintain airway contraction. ROIs were defined in single SMCs and the Ca^{2+} changes in response to ACH expressed as fluorescence ratio (top). The change in the part of the cross-sectional area of the airway that was visible in the confocal images was measured and displayed simultaneously as the delta area (bottom). Traces are representative of four to five experiments performed in different airways of different slices obtained from at least two different mice. (A) Buffering intracellular Ca^{2+} by incubation with 1 mM BAPTA-AM for 1 h prevented both, the Ca^{2+} signaling and the airway contraction in response to 10 μM ACH (bar). (B) During ongoing ACH-induced Ca^{2+} oscillations, the addition of 85 U/ml ACH-Esterase (bar) abolished the Ca^{2+} oscillations without substantially changing baseline $[Ca^{2+}]_i$ and relaxed the airway. (C) In a Ca^{2+}-free solution containing 5 mM EGTA, the addition of 10 μM ACH (bar) induced Ca^{2+} oscillations and airway contraction. However, after 1–1.5 min, the Ca^{2+} oscillations ceased and the airway relaxed. (D) 1.7 mM halothane abolished ongoing Ca^{2+} oscillations and simultaneously relaxed the airway.

tions by Ca^{2+}-free solution, the contracted airway relaxed (Fig. 10 C). Finally, the addition of 1.7 mM halothane stopped the Ca^{2+} oscillations, and this resulted in a relaxation of the airway (Fig. 10 D).

DISCUSSION

The understanding of airway SMC physiology is hampered by the inaccessibility of the cells and it is often necessary to study isolated or cultured cells. Unfortunately, this approach has several disadvantages. These include a relatively rapid change in phenotype and a loss of the SMCs contractility, the isolation of cells from central airways (e.g., trachea), rather than distal airways, and a lack of extracellular connective tissue that serves to modulate cell contraction and relaxation. In addition, it is very difficult to directly correlate changes in isolated SMC contraction with airway caliber.

To address some of these difficulties, we have refined the use of lung slices. We found that SMCs within the slice maintained the ability to perform multiple contractions for at least 5 d. These slices required minimal maintenance and appeared healthy without any special culturing conditions. Healthy lung slices also were indicated by the presence of active cilia on the airway epithelial cells. The morphology of the slice appeared, as discernible with the light microscope, unaltered with the airway epithelial cells remaining cuboidal and the SMCs remaining elongated. Obviously, some connective tissue has been disrupted at the surface of the slices, but for cells in the middle of a slice, which are accessible with confocal microscopy, their environment

approaches that of in situ. Thus, slices would appear ideal for the investigation of interactions, not only between SMCs, but also between SMCs and epithelial cells as well as the activity of individual SMCs and the response of the associated airway.

Despite these advantages, the lung slice is not without some difficulties. For example, lung slices do not adhere to the substrate and are easily displaced by experimental protocols. We have found that a piece nylon mesh can be used to hold slices in position. Lung slices also are not easily loaded with indicator dyes. This may be because the surface area of the cells in a slice that is accessible to the dye is significantly reduced by surrounding cells and connective tissue, but an increase in dye concentration and incubation time and the addition of an organic anion transporter blocker appeared to compensate for a low dye-loading rate. The process of obtaining a slice may be considered traumatic, but the process of cell isolation involves an enzymatic modification of the cell surface, a loss of cell contacts, and a lack of the connective tissue forces that mediate relaxation.

We used a higher concentration of agarose (2%) to stiffen the compliant lung tissue as compared with Dandurand et al. (1993) and Martin et al. (1996), 1% and 0.75%, respectively. The stiffer lung and the use of a precision tissue slicer or vibratome, in place of manual or hand cutting, enabled us to obtain thin slices that allow the study of single cells within the slice with confocal microscopy.

ACH-induced Airway Contraction

Many studies on airway contraction have been performed using methacholine (MCH), a chemical analogue of ACH acting via muscarinic receptors that may vary in subtype selectivity depending on species and tissue (Tulic et al., 1999). The choice to use MCH may have been based on the slower metabolism of MCH and the widespread use of MCH in clinical lung function tests. However, we choose to use ACH because ACH is readily metabolized by esterases for reversibility of experiments, contracts airway smooth muscle cells through activation of muscarinic receptors (Hall, 2000), narrows airways in lung parenchymal strips (Salerno et al., 1996) and induces Ca^{2+} oscillations in isolated tracheal SMCs (Liu and Farley, 1996; Sims et al., 1996; Prakash et al., 1997, 2000; Sieck et al., 1997).

A concentration dependence of ACH-induced airway contraction was observed in the range of 10–500 nM. At concentrations >500 nM, ACH induced maximal airway contraction, which was, on average, ~80% of the initial area. However, these results contrast to MCH-induced narrowing in thicker lung slices where increasing concentrations of MCH led to a reduction in airway lumen to <20% and complete airway closure in up to one third of the airways (Dandurand et al., 1993; Martin et al., 1996; Minshall et al., 1997). One explanation for this difference could be our use of a higher concentration of agarose to fill the lungs as compared with the previous studies because of our effort to cut thinner slices for the use with confocal microscopy. This could have increased the stiffness of the surrounding agarose-filled tissue. However, Dandurand et al. (1993) reported that 16% of the airways closed in rat lung slices when using 2% agarose. The slices used in the present study were thinner and likely to have fewer SMCs per airway. Consequently, the number of SMCs may have been insufficient to generate the force required to narrow or close airways to the same extent.

ACH-induced Ca^{2+} Signaling

The Ca^{2+} response of airway SMCs to ACH showed a biphasic pattern consisting of an initial transient followed by Ca^{2+} oscillations. ACH-induced Ca^{2+} oscillations also have been reported to occur in isolated tracheal SMCs (Liu and Farley, 1996; Sims et al., 1996; Prakash et al., 1997, 2000; Sieck et al., 1997). The oscillation frequencies in this study (~20–30 per minute) were comparable to those found for isolated tracheal SMCs (Pabelick et al., 2001b) although Sieck et al. (1997) reported slower frequencies for bronchial SMCs. We also found, like Prakash et al. (2000), a concentration dependence of the frequency of the oscillations. This concentration dependence matched that of airway contraction, and this will be addressed later.

The Ca^{2+} oscillations were found to spread through the SMCs as intracellular Ca^{2+} waves. The propagation velocity (~48 μm/s) of the Ca^{2+} waves was higher than reported by Prakash et al. (2000), who found a velocity of 25 μm/s in isolated porcine tracheal SMCs. Differences in species, airway generation, and/or the different culture form may be responsible. A comparison of the Ca^{2+} oscillations in adjacent SMCs indicated that the Ca^{2+} oscillations occurred asynchronously. If SMCs in slices communicated (e.g., via gap junctions), this did not lead to a synchronization of the Ca^{2+} oscillations. However, all the cells may have been stimulated simultaneously with extracellular ACH, and communication between cells would not be required to initiate a response in each cell. Future experiments with stimulation of single cells will be required to explore the role of cell–cell communication.

Although ACH induced Ca^{2+} oscillations in the absence of extracellular Ca^{2+}, these oscillations subsequently ceased. This indicates that an influx of external Ca^{2+} is not directly required for ACH-induced Ca^{2+} signaling, but may be necessary to refill internal Ca^{2+} stores and compensate for Ca^{2+} losses across the cell membrane. Emptying of the internal Ca^{2+} stores using thapsigargin prevented the ACH-induced Ca^{2+} response, confirming the essential role of internal Ca^{2+} release. The

abolishment of the Ca^{2+} signaling with the IP_3R antagonist xestospongin indicates that, in murine bronchial SMCs, Ca^{2+} release from the SR occurs in part via the IP_3R. Because the role of Ca^{2+} release via the RYR in agonist-induced Ca^{2+} signaling varies among SMCs of different origins (Savineau and Marthan, 2000), we tested the role of the RYR in murine bronchial SMCs using ryanodine. The ACH-induced Ca^{2+} response was blocked by ryanodine, a result indicating that in these cells Ca^{2+} release also occurs via the RYR. Taken together, we suggest, for the mechanism of ACH-induced Ca^{2+} signaling in murine bronchial SMCs, an initial small IP_3-induced Ca^{2+} release from the SR that is amplified by CICR via RYR with external Ca^{2+} influx occurring to compensate for Ca^{2+} losses to the extracellular space.

Correlation between Ca^{2+} Signaling in SMCs and Airway Contraction

Ca^{2+} contraction coupling in SMCs involves the Ca^{2+}–calmodulin complex that activates the myosin-light-chain kinase, which in turn phosphorylates the myosin-light-chain leading to crossbridge cycling and cell contraction. However, Ca^{2+}-independent pathways for agonist-induced contraction exist and these may involve diacylglycerol, CPI-17, or Rho-kinases to inhibit myosin-light-chain phosphatase, and thereby increase myosin-light-chain phosphorylation (for reviews see Somlyo and Somlyo, 2000; Pfitzer, 2001). Because we were able to inhibit the ACH-induced airway contraction with intracellular BAPTA, the ACH-induced Ca^{2+} signaling appears to directly mediate contraction in murine bronchial SMCs.

The purpose of the present study was to correlate the Ca^{2+} signaling that occurs in SMCs with airway contraction. Previously, Shieh et al. (1991) observed Ca^{2+} signaling in isolated SMCs and found that an initial Ca^{2+} transient was followed by a lower plateau of $[Ca^{2+}]_i$ at a steady state, and suggested that the Ca^{2+} transient establishes tension and that the $[Ca^{2+}]_i$ steady state maintains tension. Subsequently, Prakash et al. (2000) found that the steady state of $[Ca^{2+}]_i$, in fact, consists of Ca^{2+} oscillations, and this led them to suggest that Ca^{2+} oscillations may provide a mechanism to regulate or integrate increases in global $[Ca^{2+}]_i$. However, evidence for different contractile states at different frequencies of Ca^{2+} oscillations was not available. In our study, the ACH-induced initial Ca^{2+} transient in the SMCs occurred simultaneously with ACH-induced airway contraction, and this was followed by Ca^{2+} oscillations. It is important to note that these Ca^{2+} oscillations persisted during the maintained airway contraction.

To stop ongoing ACH-induced Ca^{2+} oscillations, we used ACH-esterase to degrade ACH, we inhibited the refilling of the Ca^{2+} stores using Ca^{2+}-free solution, or we added halothane to the bath. Pabelick et al. (2001a) could show that halothane reduces SR Ca^{2+} content by increased "leak" through IP_3- and RYR channels. In our study, halothane abolished ACH-induced Ca^{2+} oscillations after a short Ca^{2+} transient. However, in all cases, airway relaxation could be observed upon cessation of the Ca^{2+} oscillations without a substantial change in baseline $[Ca^{2+}]_i$, suggesting an essential role of Ca^{2+} oscillations in the maintenance of airway contraction.

The concentration response curves for ACH-induced Ca^{2+} oscillation frequency and airway contraction were very similar and these data may indicate a close relationship between the extent of airway contraction and the frequency of the Ca^{2+} oscillations. Similarly, in other systems, increases in the frequency of Ca^{2+} oscillations were induced by increasing concentrations of agonists and this led to the idea that frequency-encoding rather than the average $[Ca^{2+}]_i$ regulates cellular activities (for reviews see Berridge et al., 2000; Bootman et al., 2001). The hypothesis for the implementation of frequency-modulated control is that the process in question has different activation and inactivation kinetics. For example, the Ca^{2+} oscillation may serve to quickly activate the phosphorylation of the myosin-light-chain via intermediaries while inactivation via dephosphorylation may take longer. As a result, intermittent Ca^{2+} pulses could maintain a prolonged response. In conclusion, we propose that Ca^{2+} oscillations are essential for maintaining the contractile state of the airway SMCs and, thereby, the airway contraction. Further, we hypothesize that this maintenance may be frequency-modulated.

This work was supported by the National Institutes of Health grant HL49288 (to M.J. Sanderson).

Submitted: 16 November 2001
Revised: 9 January 2002
Accepted: 11 January 2002

REFERENCES

Berridge, M.J., P. Lipp, and M.D. Bootman. 2000. The versatility and universality of calcium signalling. *Nat. Rev. Mol. Cell Biol.* 1:11–21.

Bootman, M.D., T.J. Collins, C.M. Peppiatt, L.S. Prothero, L. MacKenzie, P. De Smet, M. Travers, S.C. Tovey, J.T. Seo, M.J. Berridge, et al. 2001. Calcium signalling: an overview. *Semin. Cell Dev. Biol.* 12:3–10.

Dandurand, R.J., C.G. Wang, N.C. Phillips, and D.H. Eidelman. 1993. Responsiveness of individual airways to methacholine in adult rat lung explants. *J. Appl. Physiol.* 75:364–372.

Dandurand, R.J., C.G. Wang, S. Laberge, J.G. Martin, and D.H. Eidelman. 1994. In vitro allergic bronchoconstriction in the brown Norway rat. *Am. J. Respir. Crit. Care Med.* 149:1499–1505.

Di Virgilio, F., T.H. Steinberg, and S.C. Silverstein. 1990. Inhibition of Fura-2 sequestration and secretion with organic anion transport blockers. *Cell Calcium.* 11:57–62.

Duguet, A., K. Biyah, E. Minshall, R. Gomes, C.G. Wang, M. Taoudi-Benchekroun, J.H. Bates, and D.H. Eidelman. 2000. Bronchial responsiveness among inbred mouse strains. Role of airway smooth-muscle shortening velocity. *Am. J. Respir. Crit. Care Med.* 161:839–848.

Hall, I.P. 2000. Second messengers, ion channels and pharmacology of airway smooth muscle. *Eur. Respir. J.* 15:1120–1127.

Hall, I.P., and M. Kotlikoff. 1995. Use of cultured airway myocytes for study of airway smooth muscle. *Am. J. Physiol.* 268:L1–L11.

Held, H.D., C. Martin, and S. Uhlig. 1999. Characterization of airway and vascular responses in murine lungs. *Br. J. Pharmacol.* 126: 1191–1199.

Kurosawa, H., C.G. Wang, R.J. Dandurand, M. King, and D.H. Eidelman. 1995. Mucociliary function in the mouse measured in explanted lung tissue. *J. Appl. Physiol.* 79:41–46.

Liu, X., and J.M. Farley. 1996. Acetylcholine-induced chloride current oscillations in swine tracheal smooth muscle cells. *J. Pharmacol. Exp. Ther.* 276:178–186.

Martin, C., S. Uhlig, and V. Ullrich. 1996. Videomicroscopy of methacholine-induced contraction of individual airways in precision-cut lung slices. *Eur. Respir. J.* 9:2479–2487.

Martin, C., S. Uhlig, and V. Ullrich. 2001. Cytokine-induced bronchoconstriction in precision-cut lung slices is dependent upon cyclooxygenase-2 and thromboxane receptor activation. *Am. J. Respir. Cell Mol. Biol.* 24:139–145.

Martin, C., V. Ullrich, and S. Uhlig. 2000a. Effects of the thromboxane receptor agonist U46619 and endothelin-1 on large and small airways. *Eur. Respir. J.* 16:316–323.

Martin, J.G., A. Duguet, and D.H. Eidelman. 2000b. The contribution of airway smooth muscle to airway narrowing and airway hyperresponsiveness in disease. *Eur. Respir. J.* 16:349–354.

Minshall, E., C.G. Wang, R. Dandurand, and D. Eidelman. 1997. Heterogeneity of responsiveness of individual airways in cultured lung explants. *Can. J. Physiol. Pharmacol.* 75:911–916.

Pabelick, C.M., Y.S. Prakash, M.S. Kannan, D.O. Warner, and G.C. Sieck. 2001a. Effects of halothane on sarcoplasmic reticulum calcium release channels in porcine airway smooth muscle cells. *Anesthesiology.* 95:207–215.

Pabelick, C.M., G.C. Sieck, and Y.S. Prakash. 2001b. Invited review: significance of spatial and temporal heterogeneity of calcium transients in smooth muscle. *J. Appl. Physiol.* 91:488–496.

Pfitzer, G. 2001. Invited review: regulation of myosin phosphorylation in smooth muscle. *J. Appl. Physiol.* 91:497–503.

Placke, M.E., and G.L. Fisher. 1987. Adult peripheral lung organ culture: a model for respiratory tract toxicology. *Toxicol. Appl. Pharmacol.* 90:284–298.

Prakash, Y.S., M.S. Kannan, and G.C. Sieck. 1997. Regulation of intracellular calcium oscillations in porcine tracheal smooth muscle cells. *Am. J. Physiol.* 272:C966–C975.

Prakash, Y.S., C.M. Pabelick, M.S. Kannan, and G.C. Sieck. 2000. Spatial and temporal aspects of ACh-induced $[Ca^{2+}]i$ oscillations in porcine tracheal smooth muscle. *Cell Calcium.* 27:153–162.

Salerno, F.G., H. Kurosawa, D.H. Eidelman, and M.S. Ludwig. 1996. Characterization of the anatomical structures involved in the contractile response of the rat lung periphery. *Br. J. Pharmacol.* 118:734–740.

Sanderson, M.J., and I. Parker. 2002. Video-rate confocal microscopy. *In* Methods in Enzymology. G. Marriott and I. Parker, editors. Academic Press, New York. In press.

Savineau, J.P., and R. Marthan. 2000. Cytosolic calcium oscillations in smooth muscle cells. *News Physiol. Sci.* 15:50–55.

Shieh, C.C., M.F. Petrini, T.M. Dwyer, and J.M. Farley. 1991. Concentration-dependence of acetylcholine-induced changes in calcium and tension in swine trachealis. *J. Pharmacol. Exp. Ther.* 256: 141–148.

Sieck, G.C., M.S. Kannan, and Y.S. Prakash. 1997. Heterogeneity in dynamic regulation of intracellular calcium in airway smooth muscle cells. *Can. J. Physiol. Pharmacol.* 75:878–888.

Sims, S.M., Y. Jiao, and Z.G. Zheng. 1996. Intracellular calcium stores in isolated tracheal smooth muscle cells. *Am. J. Physiol.* 271: L300–L309.

Somlyo, A.P., and A.V. Somlyo. 2000. Signal transduction by G-proteins, rho-kinase and protein phosphatase to smooth muscle and non-muscle myosin II. *J Physiol.* 522:177–185.

Tulic, M.K., J.L. Wale, F. Petak, and P.D. Sly. 1999. Muscarinic blockade of methacholine induced airway and parenchymal lung responses in anaesthetised rats. *Thorax.* 54:531–537.

Widdop, S., K. Daykin, and I.P. Hall. 1993. Expression of muscarinic M2 receptors in cultured human airway smooth muscle cells. *Am. J. Respir. Cell Mol. Biol.* 9:541–546.

Wohlsen, A., S. Uhlig, and C. Martin. 2001. Immediate allergic response in small airways. *Am. J. Respir. Crit. Care Med.* 163:1462–1469.